

Title: Synchronization of proline, ascorbate and oxidative stress pathways under the combination of salinity and heat in tomato plants

Authors: María Lopez-Delacalle¹, Christian J Silva², Teresa C Mestre¹, Vicente Martinez¹, Barbara Blanco-Ulate^{2*}, Rosa M Rivero^{1*}

(*) Corresponding authors

Addresses of the institutions:

¹ CEBAS-CSIC, Campus Universitario de Espinardo, 30100, Murcia, Spain.

² Department of Plant Sciences, University of California Davis, Davis, CA, 95616, USA.

Author's emails:

María Lopez-Delacalle: mlopez@cebas.csic.es

Christian J Silva: cjsilva@ucdavis.edu

Teresa C Mestre: tmestre@cebas.csic.es

Vicente Martinez: vicente@cebas.csic.es

Barbara Blanco-Ulate: bblanco@ucdavis.edu

Rosa M Rivero: rmrivero@cebas.csic.es

Date of Submission: June 30th 2020

N° Figures: 6

Word Count:

Supplementary material: 7 supplementary tables
3 supplementary figures.

HIGHLIGHTS:

- The combination of salinity and heat causes a unique reprogramming of tomato metabolic pathways
- Proline and ascorbate pathways act synchronously to maintain cellular redox homeostasis
- Key transcription factors were identified as putative regulators of the up-regulated genes under the combination of salinity and heat.

ABSTRACT

1 Adverse environmental conditions have a devastating impact on plant productivity. In
2 nature, multiple abiotic stresses occur simultaneously, and plants have evolved unique
3 responses to cope against this combination of stresses. Here, we coupled genome-wide
4 transcriptional profiling and untargeted metabolomics with physiological and
5 biochemical analyses to characterize the effect of salinity and heat applied in combination
6 on the metabolism of tomato plants. Our results demonstrate that this combination of
7 stresses causes a unique reprogramming of metabolic pathways, including changes in the
8 expression of 1,388 genes and the accumulation of 568 molecular features. Pathway
9 enrichment analysis of transcript and metabolite data indicated that the proline and
10 ascorbate pathways act synchronously to maintain cellular redox homeostasis, which was
11 supported by measurements of enzymatic activity and oxidative stress markers. We also
12 identified key transcription factors from the basic Leucine Zipper Domain (bZIP), Zinc
13 Finger Cysteine-2/Histidine-2 (C2H2) and Trihelix families that are likely regulators of
14 the identified up-regulated genes under salinity+heat combination. Our results expand the
15 current understanding of how plants acclimate to environmental stresses in combination
16 and unveil the synergy between key cellular metabolic pathways for effective ROS
17 detoxification. Our study opens the door to elucidating the different signaling
18 mechanisms for stress tolerance.
19
20
21
22
23
24
25
26
27
28
29
30
31
32
33
34
35

36 **Keywords:** salinity, heat, protein oxidation, lipid peroxidation, reactive oxygen species,
37 abiotic stress combination.
38
39
40
41
42
43
44
45
46
47
48
49
50
51
52
53
54
55
56
57
58
59
60
61
62
63
64
65

1 INTRODUCTION

2 Multiple environmental factors such as salinity, high temperatures, cold, or drought cause
3 abiotic stresses in plants, which result in large agricultural losses worldwide, estimated to
4 be around \$14–19 million (Rivera *et al.*, 2017). Under field conditions, different abiotic
5 stressors usually occur at the same time; for example, it is common that high temperatures
6 coexist with highly saline soils or water scarcity. Studies in the last decade have shown
7 that plant response to combined abiotic stresses are unique and cannot be deduced from
8 the study of plants subjected to each stress separately (Mittler, 2006; Miller *et al.*, 2010;
9 Rivero *et al.*, 2014; Anjum *et al.*, 2019; Sehgal *et al.*, 2019; Lopez-Delacalle *et al.*, 2020;
10 Zandalinas *et al.*, 2020).

11 Many metabolic mechanisms act in concert during the plant's response to abiotic stress,
12 including rapid changes in gene expression, ionic adjustment, and activation and
13 inactivation of proteins that carry out the synthesis and degradation of compounds used
14 for cell signaling and protection (e.g., osmoprotectants and antioxidants), among others
15 (Rivero *et al.*, 2014; Zushi *et al.*, 2014; Zandalinas *et al.*, 2020). Proline has been widely
16 reported to act as an osmoprotectant in plant defense against certain stress conditions,
17 such as drought and salinity (Rivero *et al.*, 2004b, 2014; Martinez *et al.*, 2018). Under
18 heat stress, plants synthesize proline, as reported by the induction of pyrroline-5-
19 carboxylate synthase (P5CS) and the subsequent accumulation of the amino acid (Rivero
20 *et al.*, 2004b; Torres *et al.*, 2006). Shalata & Neumann (2001) have also reported that
21 under salinity, proline accumulation can improve plant salt tolerance and reduce oxidative
22 damage by decreasing lipid peroxidation in tomato plants.

23 Stress conditions cause the accumulation of reactive oxygen species (ROS), which are
24 known to induce oxidative stress (e.g., lipid peroxidation) and serve as signaling
25 molecules in plants (Suzuki *et al.*, 2012; Kollist *et al.*, 2019). Plants accumulate
26 antioxidants, such as ascorbate (ASC), glutathione (GSH), carotenoids, tocopherols, and
27 flavonoids, and activate enzymatic reactions to maintain cell homeostasis under
28 increasing oxidative conditions. The ASC/GSH cycle is critical for detoxifying ROS from
29 plant cells. Briefly, the hydrogen peroxide (H₂O₂) generated by detoxification of
30 superoxide radicals is further converted to H₂O and O₂ by ASC peroxidase (APX), the
31 first enzyme of the ASC/GSH cycle, using ASC as an electron donor (Noctor and Foyer,
32 1998). Because ASC is considered the first antioxidant line of defense in H₂O₂
33 detoxification (Foyer and Noctor, 2011; Akram *et al.*, 2017), it is expected that plants

1
2
3
4
5
6
7
8
9
10
11
12
13
14
15
16
17
18
19
20
21
22
23
24
25
26
27
28
29
30
31
32
33
34
35
36
37
38
39
40
41
42
43
44
45
46
47
48
49
50
51
52
53
54
55
56

with a high cellular accumulation of this compound will have a greater tolerance to oxidative stress. In fact, tomato seeds treated with ascorbic acid have been shown to have better tolerance to salinity stress, improved germination, and better growth parameters (Sayed, 2013). We have previously reported (Rivero et al. 2004) that enzymes that belong to the ASC/GSH cycle were inhibited in tomato plants under high temperature, leading to H₂O₂ accumulation and inhibition of plant growth and yield. In addition to its importance in ROS detoxification, the cellular content of GSH and ASC improves osmoregulation, efficient use of water, photosynthetic activity, and general parameters of plant productivity (Noctor and Foyer, 1998; Meyer, 2008; Foyer and Noctor, 2011). Plants need to rapidly regulate and fine-tune their responses to stress to maximize energy expenditure in adverse conditions. Transcription factors (TFs) are considered key components in the control of abiotic stress signaling (Schmidt *et al.*, 2012; Castelán-Muñoz *et al.*, 2019); however, little is known about their role in stress combination. Just recently, a report by Zandalinas et al. (Zandalinas *et al.*, 2020) found that Arabidopsis plants induced a unique set of TFs when subjected to different abiotic stress combinations and that those genes were relatively unique across stress conditions. Here we hypothesize that the combination of salinity and heat induces a unique physiological response in tomato plants by activating specific regulatory and metabolic pathways that act synergistically to maintain cellular redox homeostasis. In this work, we analyze how the combination of salinity and heat affects the transcriptome and metabolome of tomato plants to find the unique elements that are differentially regulated under these stress conditions and that may be key in ROS detoxification and, thus, plant tolerance to abiotic stress combination.

57 MATERIALS AND METHODS

58 Plant material, experimental design, and growth conditions

59 *Solanum lycopersicum* L cv. Boludo (Monsanto) seeds were germinated in vermiculite
60 under optimal and controlled conditions in a growth chamber (chamber A). These
61 conditions were: a photoperiod of 16/8 hours of day/night with a light intensity of 500
62 $\mu\text{mol m}^{-2} \text{s}^{-1}$, a relative humidity (RH) between 60 and 65% and a temperature of 25 °C.
63 Subsequently, when the plants had at least two true leaves, six plants of each treatment
64 (twenty-four plants in total) were transplanted to an aerated hydroponic system containing
65 a modified Hoagland solution and grown under these conditions for one week. The
66 nutrient solution had the following composition: KNO_3 (3 mM), $\text{Ca}(\text{NO}_3)_2$ (2 mM),
67 MgSO_4 (0.5 mM), KH_2PO_4 (0.5 mM), Fe-EDTA (10 μM), H_3BO_3 (10 μM), $\text{MnSO}_4 \cdot \text{H}_2\text{O}$
68 (1 μM), $\text{ZnSO}_4 \cdot 7\text{H}_2\text{O}$ (2 μM), $\text{CuSO}_4 \cdot 5\text{H}_2\text{O}$ (0.5 μM), and $(\text{NH}_4)_6\text{Mo}_7\text{O}_{24} \cdot 4\text{H}_2\text{O}$ (0.5
69 μM) (Hoagland and Arnon, 1950). The electric conductivity (EC) and pH of the nutrient
70 solution were measured and maintained within 1.4–1.7 $\text{mS} \cdot \text{cm}^{-1}$ and 5.2–5.6,
71 respectively. After 7 days of acclimation, half of the plants were transferred to a twin-
72 chamber whose temperature was previously set at 35 °C (chamber B). In both twin
73 chambers, a saline concentration in the nutrient solution of 75 mM NaCl was added to
74 half of the plants. Therefore, four different conditions were obtained: control (25 °C and
75 0 mM NaCl), salinity (25 °C and 75 mM NaCl), heat (35 °C and 0 mM NaCl), and salinity
76 and heat (35 °C and 75 mM NaCl). Plants were kept under these conditions for 14 days.
77 After this time, six plants from each treatment were sampled for subsequent analysis. All
78 the plants were separated into roots, stems, and leaves, and fresh weight (FW) was
79 properly recorded. The leaves of each plant were immediately stored at –80 °C for
80 RNAseq, metabolomics, enzymatic activities, and oxidative metabolism-related analysis
81 as described below.

83 Measurements of photosynthetic parameters

84 Photosynthetic parameters were determined on a fully-expanded, metabolically-mature
85 middle leaf in all plants. These data were taken with a gas exchange system (LI-COR
86 6400, Li-Cor) at the beginning (day 0), the middle (day 7), and at the end of the
87 experiment (day 14). The conditions established in the LI-COR were: 1000 $\mu\text{mol photons}$
88 $\text{m}^{-2} \text{s}^{-1}$ and 400 $\mu\text{mol mol}^{-1} \text{CO}_2$. The leaf temperature was maintained at 25 °C for control
89 and salinity treatment plants, and 35 °C for plants in the high temperature, and the

1
2
3
4
5
6
7
8
9
10
11
12
13
14
15
16
17
18
19
20
21
22
23
24
25
26
27
28
29
30
31
32
33
34
35
36
37
38
39
40
41
42
43
44
45
46
47
48
49
50
51
52
53
54
55
56
57
58
59
60
61
62
63
64
65

90 combination of high temperature and salinity treatments. The leaf-air vapor pressure
91 deficit was maintained between 1-1.3 kPa. With this analysis, the device reported data on
92 CO₂ assimilation, stomatal conductance, and transpiration rate. At the end of the
93 experiment, the leaves, stem, and root were separated, and the fresh weight (FW) of each
94 part of the plant was determined separately.

96 **Quantification of oxidative stress-related markers**

97 *H₂O₂ accumulation*

98 H₂O₂ was extracted from leaves of six plants at the end of the experiment (day 14) as
99 described by Yang et al. (2007), with some modifications, which are fully described in
100 García-Martí et al. (García-Martí *et al.*, 2019). These samples (n=6) were used for the
101 future determination of H₂O₂ concentration and lipid peroxidation. H₂O₂ was quantified
102 as described by MacNevin and Urone (1953).

103 *Lipid peroxidation*

104 For lipid peroxidation determination, malondialdehyde (MDA) was used, which is a
105 product of the peroxidation of membrane lipids. The same enzyme extract as the one
106 utilized for the determination of H₂O₂ was used. The procedure was described by Fu and
107 Huang (2001).

108 *Antioxidant capacity*

109 Regarding antioxidant capacity, it was carried out according to the protocol by Koleva *et*
110 *al.* (2002). The remaining amount of 2,2-diphenyl-1-picrylhydrazyl (DPPH), measured at
111 a certain time, is inversely proportional to the antioxidant capacity of the substances
112 present in the sample. Results are expressed as % Radical Scavenging Activity (RSA), or
113 percentage of free radical scavenging activity.

114 *Protein oxidation*

115 Protein oxidation was assayed according to Reznick and Packer (1994). PCO groups react
116 with 2,4-dinitrophenylhydrazine (DNPH) to generate chromophoric
117 dinitrophenylhydrazones, which can be recorded with a spectrophotometer. The
118 absorbance was measured at 360 nm, using the molar extinction coefficient of DNPH
119 $2.2 \times 10^4 \text{ M}^{-1} \text{ cm}^{-1}$.

120 **RNA extraction and sequencing**

121 Total RNA was extracted from 1 g of frozen tomato leaves using TRI-Reagent (Sigma-
122 Aldrich) and following the manufacturer's instruction. The quantity and quality of RNA

123 were determined using a NanoDrop 3300 fluorospectrometer (Thermo Scientific
124 Instruments, USA). Three biological replications for each treatment were used for total
125 RNA extraction and sequencing. For each RNA sample, mRNA was enriched using a
126 Dynabeads mRNA purification kit (Invitrogen), then the samples were sent to BGI-
127 Shenzhen (hereafter 'BGI', China) for RNA sequencing. Sequencing was carried out on
128 a HiSeq2000 according to the Illumina protocols for 90×2 pair-end sequencing covering
129 a read length of 100 bp. An average of 10 Gb clean data per sample was generated after
130 filtering to ensure a complete set of expressed transcripts with sufficient coverage and
131 depth for each sample.

132

133 **Bioinformatics pipeline**

134 *RNA sequencing and data processing*

135 Raw sequencing reads were trimmed for quality and adapter sequences using
136 Trimmomatic v0.33 (Bolger *et al.*, 2014) were used with the following parameters:
137 maximum seed mismatches = 2, palindrome clip threshold = 30, simple clip threshold =
138 10, minimum leading quality = 3, minimum trailing quality = 3, window size = 4, required
139 quality = 15, and minimum length = 36. Trimmed reads were mapped using Bowtie2
140 (Langmead and Salzberg, 2012) to the tomato transcriptome (SL4.0 release;
141 <http://solgenomics.net>). Count matrices were made from the Bowtie2 results using
142 sam2counts.py v0.91 (<https://github.com/vsbuffalo/sam2counts/>). A summary of the
143 quality assessment and mapping results can be found in **Supplementary Table S1**. The
144 raw sequencing reads and the read mapping count matrices are available in the National
145 Center for Biotechnology Information Gene Expression Omnibus database under the
146 accession GSE152620.

147 *Differential expression analysis*

148 The Bioconductor package DESeq2 (Love *et al.*, 2014) was used to perform
149 normalization of read counts and differential expression analyses for various treatment
150 comparisons. Differentially expressed (DE) genes for each comparison were those with
151 an adjusted p-value of less than or equal to 0.05.

152 *Functional annotation and enrichment analyses*

153 Basic functional annotations for genes were determined with the Automated Assignment
154 of Human Readable Descriptions (AHRD) provided in the SL4.0 build of the tomato
155 genome. KEGG annotations were determined using the KEGG Automatic Annotation

156 Server (Moriya *et al.*, 2007). Enrichments were conducted via Fisher's exact test with p-
157 values adjusted using the Benjamini and Hochberg method (Benjamini and Hochberg,
158 1995).

159 *Promoter motif analysis*

160 Binding motifs for tomato transcription factors were obtained from the Plant
161 Transcription Factor Database (<http://planttfdb.cbi.pku.edu.cn/>). Promoter sequences
162 defined as 1000 base pairs upstream from the transcription start site of each gene were
163 obtained using the 'flank' function in bedtools v2.29.2
164 (<https://bedtools.readthedocs.io/en/latest/>). Enrichment of transcription factor binding
165 motifs on the promoter sequences of up-regulated genes was performed using the
166 Analysis of Motif Enrichment tool in MEME-Suite (McLeay and Bailey, 2010) using all
167 non-up-regulated tomato genes as the control sequences, the average odds score scoring
168 method and Fisher's exact test.

169

170 **Metabolomics analysis**

171 Six biological replications of frozen tomato leaves per treatment were used for the
172 metabolomics analysis. One gram of this frozen plant material was extracted in methanol:
173 water (3:1 v/v) as described previously in Martinez *et al.* (2016). Agilent MassHunter
174 Qualitative analysis software v 6.00 (Agilent Technologies, Palo Alto, USA) was used to
175 obtain an initial peak processing (**Supplementary Fig. S1**). Then, XCMS online software
176 (www.xcmsonline.scripts.edu) which incorporates CAMERA (a Bioconductor package
177 to extract spectra, annotate isotopes and adduct peaks, among other functions) in its
178 analysis, was implemented in our curated raw data (**Supplementary Table S2**). A second
179 level of statistical analysis was carried out, consisting of data normalization of the peaks
180 obtained for each treatment against the control, and a t-test followed by an ANOVA
181 analysis. Then, \log_2 of the fold-change was calculated and all the molecular features with
182 a P_{adj} adjusted greater than 0.05 and a \log_2 fold change (FC) greater than -1 or smaller
183 than 1 were eliminated from the analyses (**Supplementary Table S3**). All the molecular
184 features that remained after these restricted statistical analyses were compared among the
185 different treatments applied (supplementary Table S3; Euler diagram Fig 3B).

186 The metabolite identification of the molecular features of interest for this study was
187 performed using a mathematical search based on the predicted elemental composition
188 through some of the most important open-source databases (MOTO, KNApSAcK,

189 KOMOCS, MassBank, ARMeC and METLIN) within a mass tolerance of 10 ppm. Then,
190 the isotope ratio (IR) and retention time (rt) from the different metabolites identified
191 unequivocally were checked again across the different databases mentioned above.
192 Identified metabolites that remained after this filtering were labeled accordingly and
193 highlighted in yellow in **Supplementary Table S4**. The concentration of the compounds
194 that showed significant differences ($P_{adj} < 0.05$ and $\log_2 FC > 2$) under salinity and heat
195 combination as compared to control plants and which were of interest in this study were
196 plotted in a box-and-whisker type plot using XCMS online (**Supplementary Figs. S2**
197 **and S3**).

198 **Enzymatic activities**

199 *Crude extract*

200 All enzymatic activities were extracted from six biological replicates of tomato leaves at
201 the end of the experiment (day 14) according to the procedure described by Torres *et al.*
202 (2006).

203 *Superoxide dismutase (SOD)*

204 SOD activity was assayed as described previously by McCord JM (1969). SOD activity
205 was expressed as units of SOD (mg prot)⁻¹ (min)⁻¹, a unit which indicates the amount of
206 enzyme needed to neutralize one unit of xanthine oxidase.

207 *Catalase (CAT)*

208 CAT activity was calculated using the extinction coefficient of 39.4 mM⁻¹cm⁻¹ as
209 described by Aebi (1984). CAT activity was expressed as μmol of reduced H₂O₂ (mg
210 prot)⁻¹ (min)⁻¹.

211 *Ascorbate peroxidase (APX) Dehydroascorbate reductase (DHAR) and* 212 *Monodehydroascorbate reductase (MDHAR)*

213 APX, DHAR and MDHAR activities were assayed as described by Miyake and Asada
214 (1992). The rate of reaction was calculated using a molar extinction coefficient of 2.8
215 mM⁻¹ cm⁻¹. APX activity was expressed as μmol of reduced ascorbic acid (mg prot)⁻¹
216 (min)⁻¹.

217 *Glutathione peroxidase (GPX)*

218 GPX activity was carried out using the Glutathione Peroxidase Assay Kit (Abcam, Ref.
219 ab102530, Cambridge, UK) considering the decrease of NADPH at 340 nm, using an
220 extinction coefficient of 6.22 mM⁻¹ cm⁻¹.

222 *Glutathione reductase (GR)*

223 GR activity was assayed through the non-enzymatic NADPH oxidation (Halliwell and
224 Foyer, 1976). The activity was determined by measuring the decrease in the reaction rate
225 at 340nm and was calculated from the 6.22 mM⁻¹ extinction coefficient.

226 *Protein concentration in the enzyme extract*

227 Proteins were quantified with the Bradford method (Bradford, 1976), in which a volume
228 of Bradford Reagent reagent (BioRAD, Catalog No. 30214) was added to an aliquot of
229 the enzyme extract. The absolute values, as well as the calculated log₂ of the data
230 normalized against control plants of all the enzymatic activities assayed, can be found in
231 **Supplementary Table S5**.

233 **Statistical analysis**

234 Statistical analysis for FW, photosynthetic parameters, H₂O₂ concentration, MDA
235 content, protein oxidation, and enzymatic activities was performed with an analysis of
236 variance with p-value < 0.05 set as the cut-off value, as indicative of significant
237 differences, followed by a Duncan test and a t-test when necessary. Transcriptomics and
238 metabolomics statistical analysis was performed as described above.

240 **RESULTS**

241 **Tomato plants grown under the combination of salinity and heat showed a better
242 performance in the photosynthetic parameters as compared to salinity alone**

243 Eighty-four tomato plants were grown in two independent chambers using four different
244 environmental conditions: 25 °C and 0 mM NaCl (control), 25 °C and 75 mM NaCl
245 (salinity), 35 °C and 0 mM NaCl (heat), and 35 °C and 75 mM NaCl (heat + salinity) for
246 14 days (**Fig. 1A**). Fresh weight was recorded at the end of the experiment (**Fig. 1B**).
247 Salinity and the salinity + heat resulted in a significant reduction of biomass when
248 compared to control plants, whereas the heat-treated plants did not differ significantly
249 from the controls. Interestingly, when salinity and heat were applied simultaneously, the
250 growth was significantly improved as compared to salinity up to about 18%.
251 Photosynthetic parameters were also measured at 0 days, and after 7 and 14 days after the
252 start of the treatments, as stress physiological markers (**Figs. 1C-F**). In our experiments,
253 CO₂ assimilation rate was highly inhibited after 7 days under salinity as compared to
254 control plants, with an inhibition of 50% at 7 days, and 70% at 14 days with respect to

1
2
3
4
5
6
7
8
9
10
11
12
13
14
15
16
17
18
19
20
21
22
23
24
25
26
27
28
29
30
31
32
33
34
35
36
37
38
39
40
41
42
43
44
45
46
47
48
49
50
51
52
53
54
55
56
57
58
59
60
61
62
63
64
65

255 control plants (**Fig. 1C**). The other stress treatments applied (heat and salinity + heat) did
256 not differ significantly as compared to the values obtained in control plants during the
257 entire experiment, contrary to that observed under salinity. Control plants had a
258 transpiration rate and a stomatal conductance that were practically constant during the
259 entire experiment, whereas plants subjected to heat and salinity + heat treatments showed
260 a significant increase in transpiration rate (41%) and stomatal conductance (29%) at 7
261 days, which was maintained until the end of the experiment (**Figs. 1D and 1E**).
262 Contrarily, the salinity treatment led to a significant reduction in the transpiration rate and
263 the stomatal conductance at day 7 from the start of the treatment until the end. In this
264 regard, the salinity + heat treatment showed a significant improvement in the
265 photosynthetic parameters as compared to salinity alone. Curiously, no differences were
266 found between salinity, heat, and the combination of both stresses for water use efficiency
267 (WUE, **Fig. 1F**), but all the treatments showed a significant decrease in this parameter as
268 compared to control plants.

269

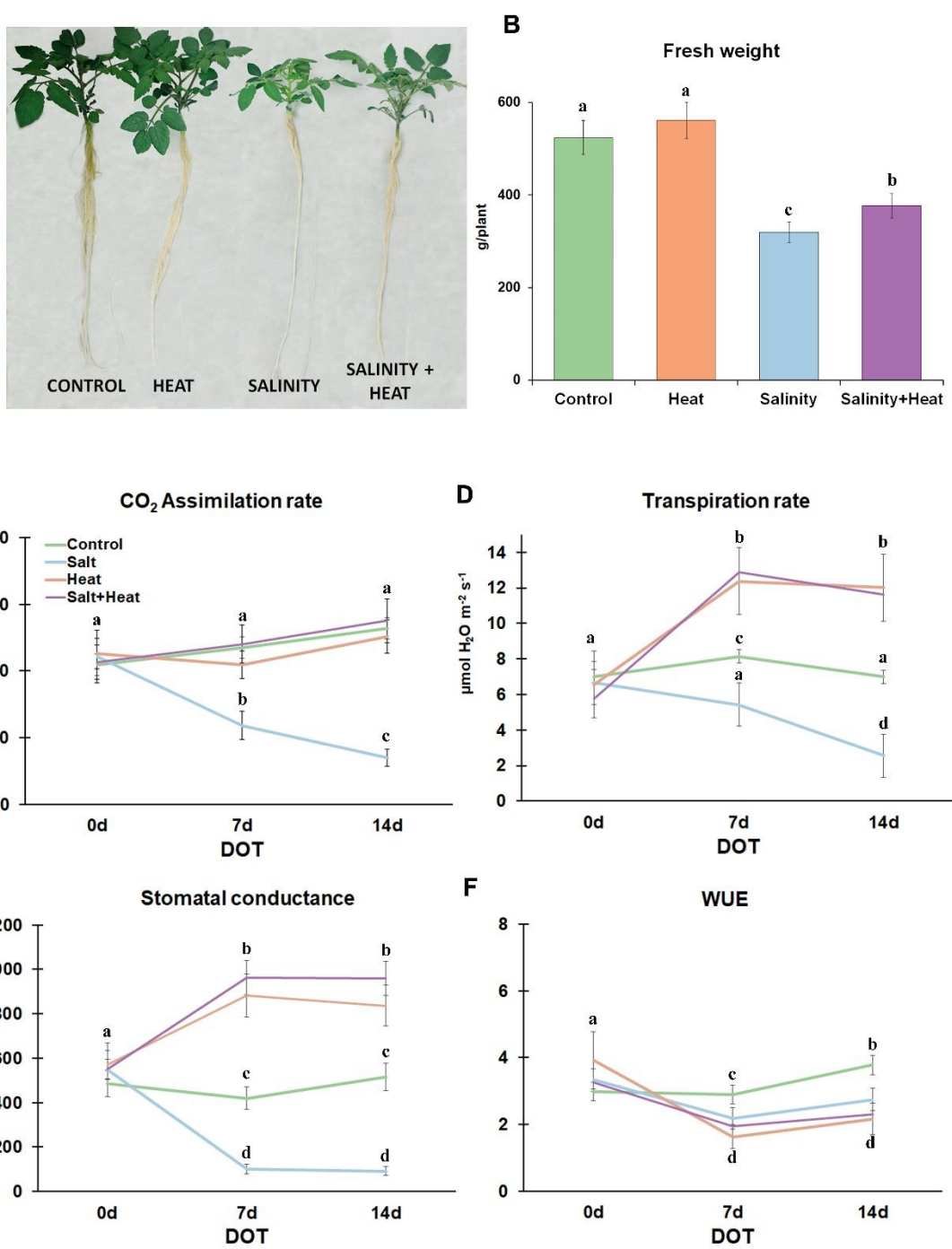


Figure 1. (A) Pictures of tomato plants at the end of the control or stress treatments. (B) Whole plant fresh weight (FW) of tomato plants grown under control, heat, salinity or the combination of salinity and heat. (C-F) Photosynthetic parameters measured in the third and four fully mature expanded leaves of tomato plants grown under control or stress conditions measured at the beginning (0 days), during (7 days) or at the end (14 days) of the treatments. Values represent means \pm SE (n = 9). Bars with different letters within each panel are significantly different at $p < 0.05$ according to Tukey's test. WUE: water use efficiency; DOT: days of treatment.

270
271
272

273 **Salinity and heat combination induced a specific transcriptional response and**
274 **pathway activation**

275 An RNAseq study was performed to identify specific biochemical pathways or molecular
276 functions that could explain the different physiological responses of the tomato plants to
277 the salinity, heat, and salinity + heat treatments. RNA was sequenced from three
278 biological replicates from each treatment, including control plants. A principal
279 component analysis of the normalized reads revealed that all samples clustered according
280 to treatment, which validated the unique transcriptional reprogramming caused by each
281 stress condition (**Fig. 2A**). Then, differential expression analysis was performed to
282 determine the individual genes affected by each treatment when compared to the control.
283 A total of 15,852 genes were found to be differentially expressed ($P_{adj} < 0.05$) across all
284 three treatments (**Supplementary Table S6**). A comparison of both up- and down-
285 regulated genes from each of the three treatments further confirmed that each treatment
286 resulted in a high number of unique differentially expressed genes (**Fig. 2B**). Most
287 notably, it was found that 1,388 (7.32% of the total) were differentially expressed only
288 for salinity + heat, with 923 genes up-regulated and 465 genes down-regulated by this
289 stress combination (**Fig. 2B**).

290 To identify important functions activated in response to each stress, an enrichment
291 analysis of the significantly up-regulated genes was conducted using pathway annotations
292 from the Kyoto Encyclopedia of Genes and Genomes (KEGG; **Supplementary Table**
293 **S7**). A total of 27 pathways were found to be enriched ($P_{adj} < 0.05$) with these up-
294 regulated genes across the three treatments (**Fig. 2C**). In line with the genes themselves,
295 enriched pathways were largely enriched in just one of the three treatments, except for
296 three pathways (glutathione metabolism (sly00480), protein processing in the ER
297 (sly04141), and spliceosome (sly03040)). Most interestingly, the salinity+heat treatment
298 resulted in the upregulation of genes belonging to two main metabolic pathways, ASC
299 and aldarate metabolism (sly00053) and arginine and proline metabolism (sly00330),
300 which were not enriched in either of the individual stress treatments, suggesting that the
301 combination of stresses induced specific changes in plant metabolism that in turn led to
302 variation in the physiological responses of the plants.

303

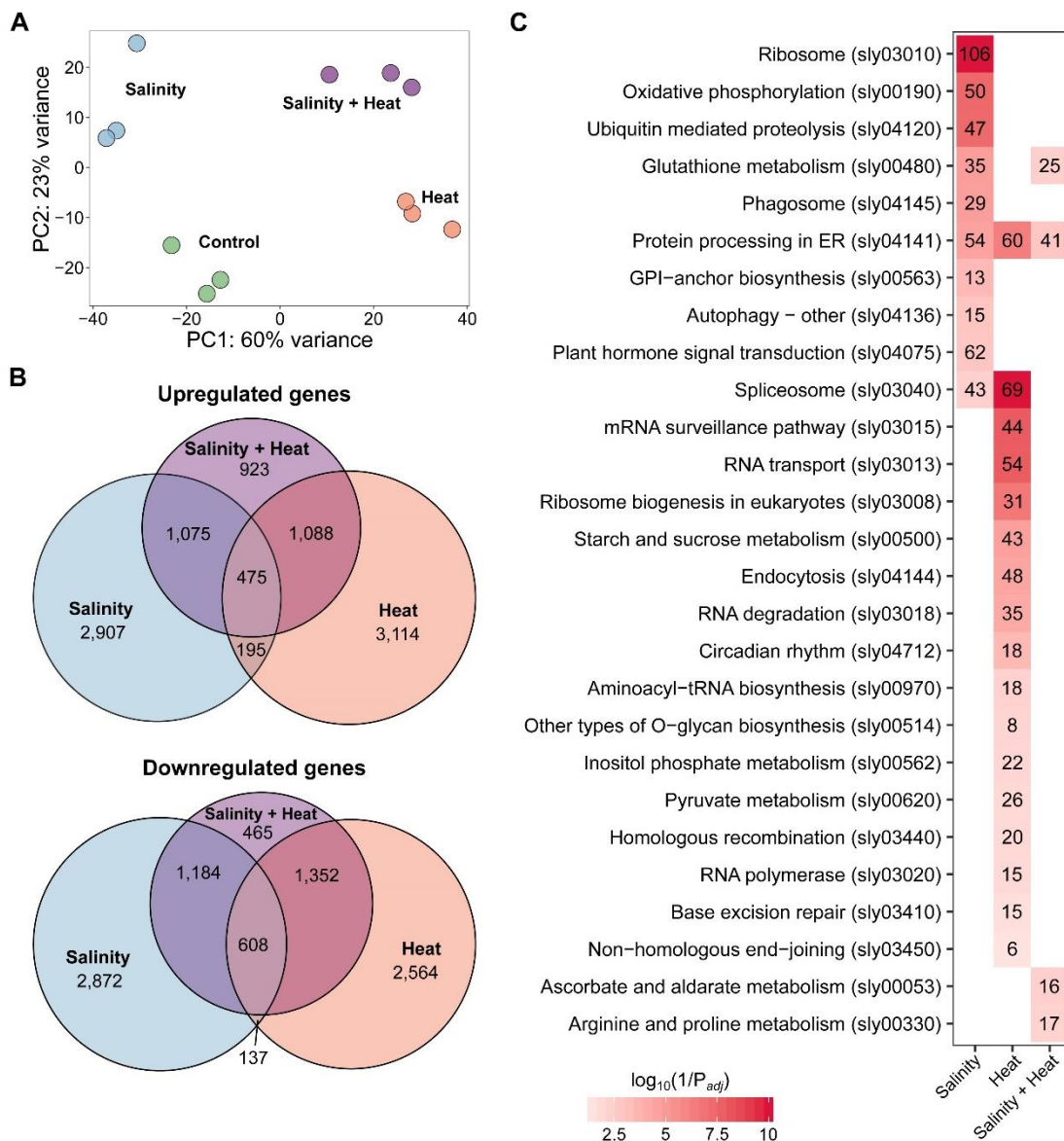


Figure 2. RNAseq analysis performed in tomato leaves after 14 days of growing under control or stress (salinity, heat or the combination of salinity and heat) conditions. **(A)** Principal component analysis (PCA) of the normalized reads obtained for each treatment. **(B)** Euler diagram representing up- and down-regulated genes (adjusted $P < 0.05$) of tomato plants grown under control, simple (salinity or heat) or combined (salinity + heat) stress. **(C)** Pathway enrichment analysis performed within the up-regulated genes under the different stress conditions applied. The scale is the $\log_{10}(1/P_{adj})$, with redder colors indicating greater statistical significance. Values greater than 10 were converted to 10 for scaling purposes. More details on these analyses can be found in the Materials and Method section.

The salinity and heat combination showed a unique metabolic profile with the enrichment of specific pathways

A metabolomics study was carried out to identify molecular features that were common or unique to the simple or combined stresses and to validate the RNAseq results. Our

1
2
3
4
5
6
7
8
9
10
11
12
13
14
15
16
17
18
19
20
21
22
23
24
25
26
27
28
29
30
31
32
33
34
35
36
37
38
39
40
41
42
43
44
45
46
47
48
49
50
51
52
53
54
55
56
57
58
59
60
61
62
63
64
65

310 main interest mainly resided in those that were specifically accumulated under the
311 combination of salinity and heat. A total of 3,338 molecular features showed significant
312 ($P_{adj} < 0.05$ and a $\log_2 < -1$ or $\log_2 > 1$) changes across the three stress conditions. Similar
313 to the RNAseq analyses, each stress condition showed a unique metabolic profile (**Fig.**
314 **3A; Supplementary Tables S3 and S4**). Only 208 molecular features were commonly
315 altered by all the treatments, which represented 6.30% of the total. When the combination
316 of salinity and heat was applied, a total of 568 molecular features (17.19% of the total)
317 were significantly and specifically accumulated as compared to control (**Fig. 3B**). Salinity
318 + heat caused reprogramming of multiple metabolic pathways, observed as a similar
319 number of molecular features that were up- or down-regulated, 337 and 208, respectively
320 when compared to the control (**Fig. 3C**). Pathway enrichment analysis of the up-regulated
321 molecular features revealed that four biochemical pathways (i.e., ASC and aldarate
322 metabolism, purine metabolism, arginine and proline metabolism and arginine
323 biosynthesis) were significantly altered in tomato under the combination of salinity and
324 heat (**Fig. 3D and Supplementary Table S4, Supplementary Figs. S2 and S3**). In
325 agreement with the RNAseq data, the ASC and aldarate metabolism and the arginine and
326 proline metabolism were among the most significantly enriched pathways.

1
2
3
4
5
6
7
8
9
10
11
12
13
14
15
16
17
18
19
20
21
22
23
24
25
26
27
28
29
30
31
32
33
34
35
36
37
38
39
40
41
42
43
44
45
46
47
48
49
50
51
52
53
54
55
56
57
58
59
60
61
62
63
64
65

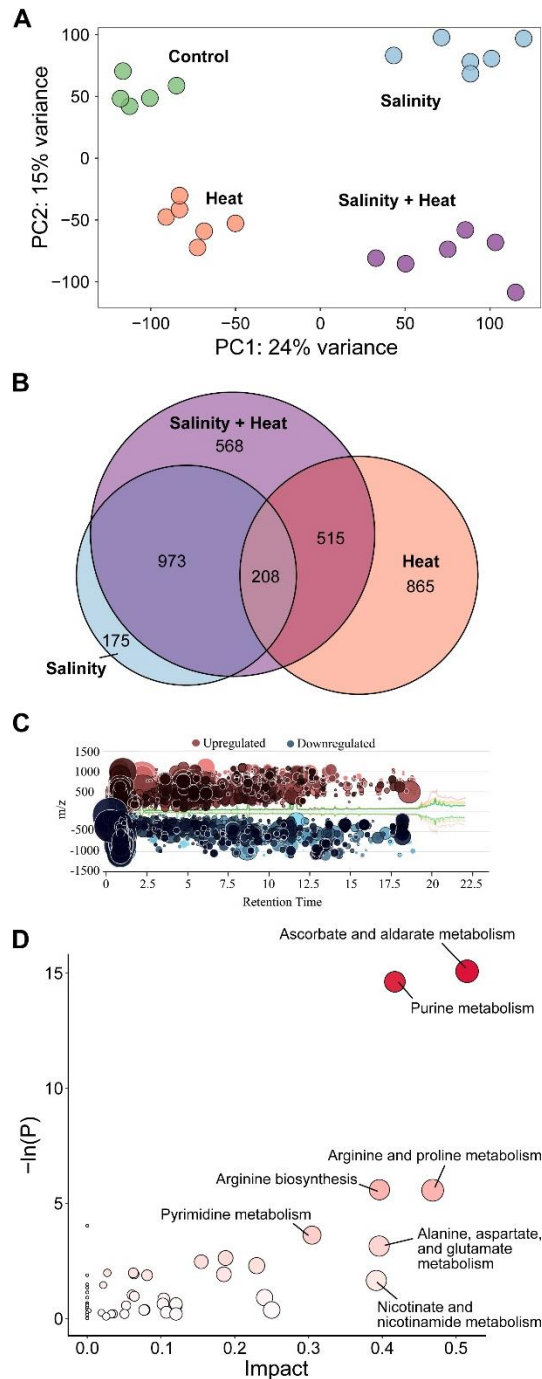


Figure 3. Metabolomic analysis performed in tomato leaves after 14 days of growing under control, simple (salinity or heat) or combined (salinity + heat) stress conditions. **(A)** Principal component analysis (PCA) of the normalized molecular features found under each treatment applied ($n = 6$). **(B)** Euler diagram of the common and uniquely molecular features with a differential and significant accumulation in each treatment ($P_{adj} < 0.05$). **(C)** Bubble diagram representing the up- and down-regulated molecular features found among the 568 molecular features uniquely and significantly changing under the combination of salinity + heat. Each bubble (i.e. molecular feature) is positioned in the chromatogram by its mass-to-charge (y-axis) and retention time (x-axis) and the size and darkness of one bubble represented the \log_2 and p-value, respectively of this molecular feature. The raw data of Figure 3C can be found in the supplemental material (Supplementary Table S2 and S3). **(D)** KEGG pathway enrichment analysis performed with the significantly up-regulated molecular features identified under the combination of salinity + heat. More details on these analyses can be found in the Materials and Methods section.

327

328

329 **The integration of transcriptomics and metabolomics revealed that the proline and**
330 **ASC pathways are interconnected for ROS homeostasis**

331 The RNAseq and metabolomics data were combined with measurements of enzymatic
332 activity to obtain a detailed picture of the changes in the ASC and aldarate, and arginine
333 and proline metabolic pathways caused by the combination of salinity and heat stresses
334 (**Fig. 4**). The first observation was that proline appears to be degraded in favor of 4-
335 hydroxyproline and L-glutamate-5-semialdehyde accumulation, with the concomitant up-
336 regulation of prolyl 4-hydroxylase (P4HA) and pyrroline-5-carboxylate reductase
337 (PROC), as well as the down-regulation of proline dehydrogenase (PRODH). The
338 accumulation of L-glutamate-5-semialdehyde was also likely derived from ornithine
339 through the up-regulation of arginase (ARG) and ornithine aminotransferase (ROCD). In
340 summary, proline was not differentially accumulated under the combination of salinity +
341 heat as compared to controls. Instead, 4-hydroxyproline and L-glutamate-5-
342 semialdehyde, two proline-derivative compounds, significantly accumulated in tomato
343 leaves under stress combination.

344 ASC significantly accumulated under combined salinity and heat stress in tomato. Its
345 synthesis from UDP-glucose or myo-inositol results in the precursor D-glucuronate,
346 which also increased under salinity + heat, in part due to the down-regulation of
347 glucuronokinase transcript (GLCAK) through glucuronate-1P synthesis and to the up-
348 regulation of one copy of the inositol oxygenase (MIOX). The levels of L-gulose and L-
349 gulonate also increased under the combination of stresses, which seemed to favor ASC
350 accumulation. The high ASC levels observed in tomato plants under stress combination
351 could also be due to the degradation of the GDP-L-galactose and L-galactose-1P, since
352 GDP-L-galactose phosphorylase (VTC2-5) and L-galactose 1-phosphate phosphatase
353 (VTC4) were up-regulated under these conditions (**Fig. 4**). ASC is known to detoxify
354 ROS through the Halliwell-Asada cycle. Remarkably, this pathway was highly
355 represented among the differentially expressed genes and the significant molecular
356 features altered by salinity + heat (**Figs. 2-3**). These results were also supported by the
357 enzymatic activities of the proteins encoded by those transcripts (**Fig. 4**). Superoxide
358 dismutases (SOD1 and SOD2), involved in cell ROS detoxification, were up-regulated at
359 the transcript and activity levels, leading to the conversion of $O_2^{\cdot -}$ to H_2O_2 . Then, H_2O_2
360 can be detoxified by catalase (CAT) or by ASC peroxidase (APX) through the ASC/GSH
361 pathway. CAT was not differentially expressed in the RNAseq analysis and the enzyme

1
2
3
4
5
6
7
8
9
10
11
12
13
14
15
16
17
18
19
20
21
22
23
24
25
26
27
28
29
30
31
32
33
34
35
36
37
38
39
40
41
42
43
44
45
46
47
48
49
50
51
52
53
54
55
56
57
58
59
60
61
62
63
64
65

362 activity was inhibited by stress combination. Several APX homologs were up-regulated
363 at the transcript level and, more importantly, its enzymatic activity was very high ($\log_2 =$
364 1.97, **Supplementary Table S5**) under salinity + heat. The APX activity generates
365 monodehydroascorbate, which accumulated significantly in our experiments.
366 Monodehydroascorbate spontaneously forms dehydroascorbate, which is reduced to
367 ASC, once again through the action of dehydroascorbate reductase (DHAR), using
368 glutathione (GSH) as a reducing agent. Tomato plants showed a significant accumulation
369 of glutathione and monodehydroascorbate under combined salinity and heat stress, with
370 a non-significant dehydroascorbate accumulation or DHAR activity. However, the
371 MDAR enzyme, responsible for the regeneration of ASC, was up-regulated at the
372 transcript and enzymatic levels. Lastly, the glutathione peroxidases GPX and PhGPX,
373 responsible for the recovery of lipid peroxidation, were also up-regulated under stress
374 combination. Our results are indicative of a connection between ASC synthesis and
375 oxidative stress-proline metabolism, with the intersection between these pathways found
376 at the 1-pyrroline-5-carboxylate level (**Fig. 4**).

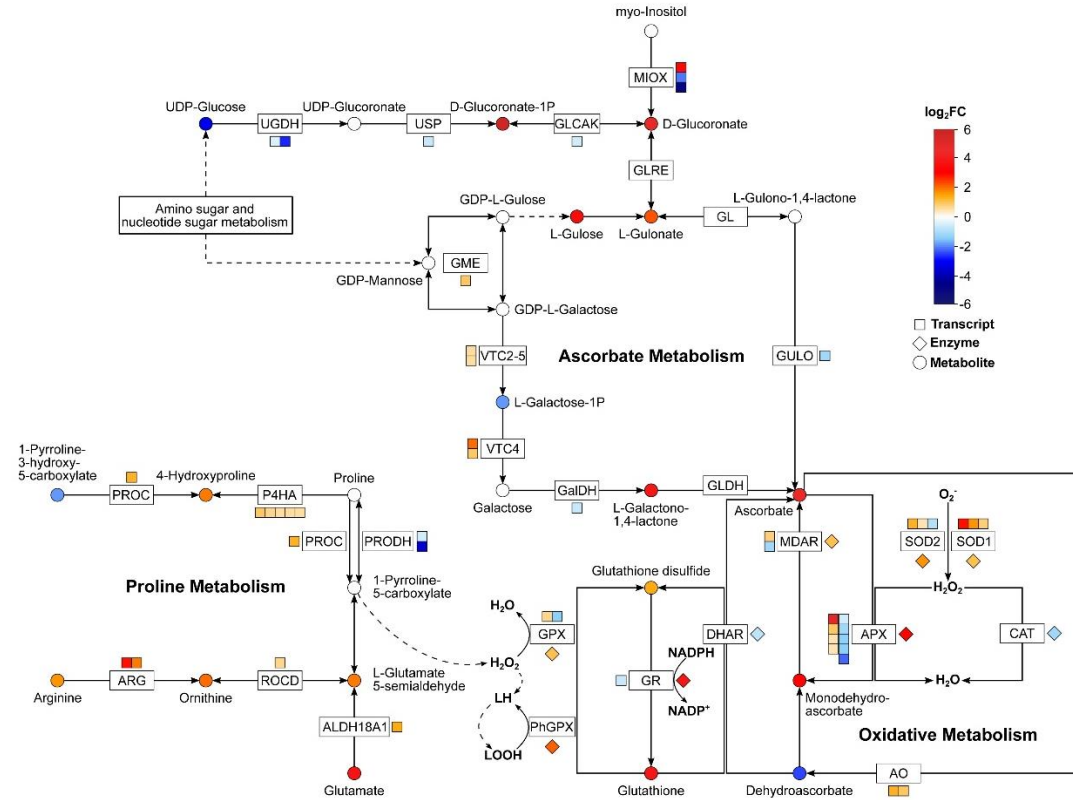


Figure 4. Schematic diagram of the metabolic interconnection between ascorbate, proline and oxidative metabolism in tomato plants. Log₂(fold change) of the metabolite concentration (○), gene expression (□) or enzymatic activity (◇) obtained in tomato plants grown under the combination of salinity + heat after RNAseq, metabolomics or biochemical analyses were represented. The data represented for genes, metabolites and enzymatic activities were obtained by comparison with the control treatment. Row data and specific information can be found in Material and Methods section and in the Supplementary material.

377

378

379 **Plants subjected to salinity and heat combination showed lower oxidative damage** 380 **than those under salinity alone**

381 The proposed coordination between the proline, ASC, and redox pathways may improve
382 the ability of the tomato plants to deal with ROS detoxification. Markers of oxidative
383 stress were evaluated to determine if tomato plants subjected to stress combination
384 displayed a more efficient antioxidant system than those plants grown under individual
385 stresses (**Fig. 5**). Tomato plants under salinity had the highest levels of H₂O₂, with a
386 significant 4-fold increase compared to control plants. However, when salinity and heat
387 were applied in combination, it was found that the H₂O₂ content was about 50% lower
388 than in the salinity treatment (**Fig. 5A**). A similar trend was observed for lipid
389 peroxidation, an indicator of oxidative damage to cell membranes, with a maximum value

390 found for salinity stress, and an intermediate value found for the salinity + heat stress
391 combination (**Fig. 5B**). Thus, the stress combination appears to reduce oxidative damage
392 as compared to the salinity treatment. In neither case, the differences between heat stress
393 and control were statistically significant. Interestingly, the antioxidant capacity (**Fig. 5C**)
394 obtained for plants subjected to salinity was the lowest among all treatments, with a
395 reduction of up to 90% as compared to the controls. When salinity and heat were
396 combined, the antioxidant capacity index was significantly lower than the control but 6-
397 fold higher than salinity. Again, the heat treatment did not show significant differences
398 respect to control. Protein oxidation values obtained for the four stress conditions were
399 directly related to H₂O₂ and lipid peroxidation, with a positive and significant correlation
400 (H₂O₂-protein oxidation: $r = 0.992$, $P_{adj} < 0.001$; lipid peroxidation-protein oxidation: $r =$
401 0.996 , $P_{adj} < 0.001$). In short, our results indicated that ROS levels were lower when
402 salinity and heat were applied jointly as compared to the salinity treatment alone, which
403 was directly observed as a lower damage to the membrane lipids and to the cellular
404 proteins under abiotic stress combination.

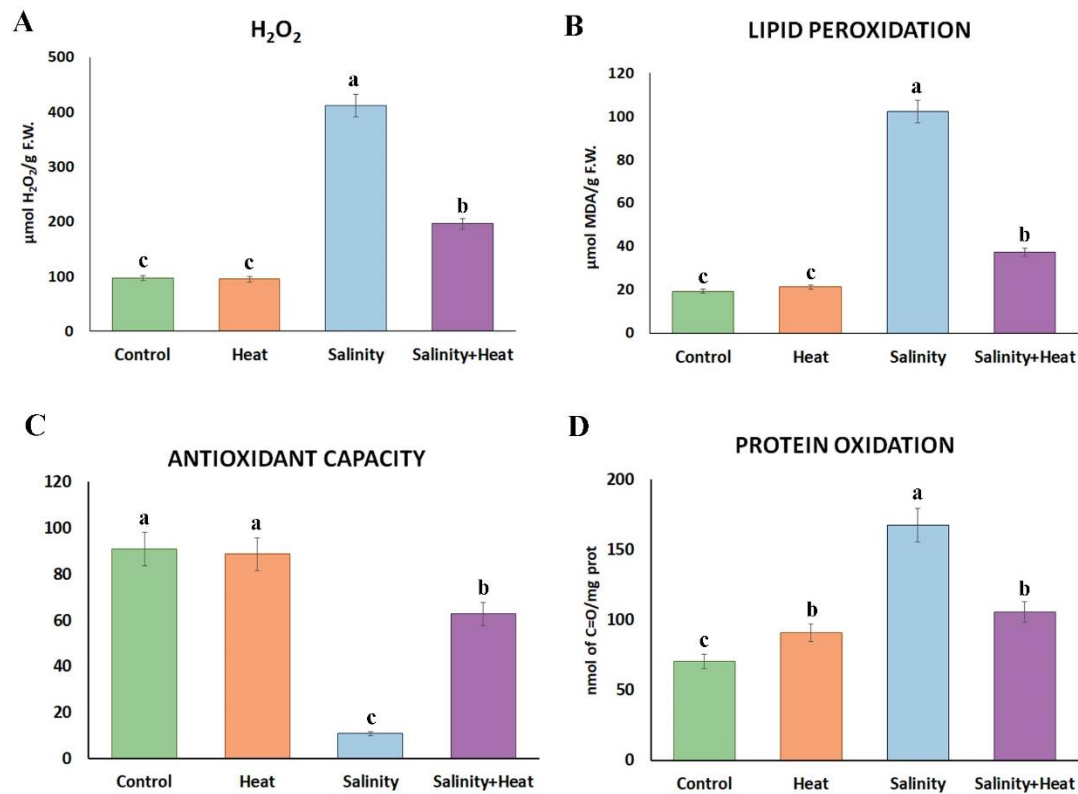


Figure 5. Oxidative metabolism-related markers measured in tomato leaves grown for 14 days under control, simple (salinity +heat) or combined (salinity+heat) stress. Values represent means \pm SE (n = 6). Bars with different letters within each panel are significantly different at $p < 0.05$ according to Tukey's test.

The combined salinity and heat responses are associated with the upregulation of unique transcription factors families

The high specificity of the tomato plant responses to salinity + heat suggests that a tight regulatory control must be in place to rapidly and efficiently cope with the oxidative damage caused by these conditions. TFs are known to be key players in modulating the expression of genes involved in abiotic stress responses. TFs that may regulate the transcriptional responses to salinity, heat, and/or salinity + heat were identified by evaluating the promoter regions (1000 bp upstream from the transcription start site) of up-regulated genes from each stress condition for overrepresented cis-element motifs (**Fig. 6A**). Binding sites from a total of 46 TFs belonging to multiple gene families were found to be enriched ($P_{adj} < 0.05$) across all treatments. Of these, only 9 TFs were associated with all stress conditions (salinity, heat, and salinity + heat), including three Homeobox-Homeodomain-Leucine Zipper Protein (HB-HD-ZIP) TFs identified. The

420 salinity + heat treatment exhibited five unique TFs, including three from the stress-related
421 Zinc Finger Cysteine-2/Histidine-2 (C2H2) family.

422 In contrast to the diverse enrichment results, most enriched TFs did not exhibit significant
423 up-regulation themselves under their associated stress condition. For salinity + heat, only
424 three TFs had significant ($P_{adj} < 0.05$) expression levels when compared to the controls
425 (**Fig. 6B**). These TFs, one each from the basic Leucine Zipper Domain (bZIP), C2H2, and
426 HB-HD-ZIP families, were also all differentially expressed in the salinity treatment,
427 although the bZIP TF (*Solyc04g078840*) was down-regulated under this treatment, and
428 up-regulated exclusively for salinity + heat. None of these three were differentially
429 expressed under the heat stress alone. The sequences of the differentially expressed genes
430 from the proline, ASC, and redox pathways (**Fig. 4**) were evaluated to determine which
431 of the overrepresented cis-element motifs associated with salinity + heat were present in
432 their promoters (**Fig. 6A**). Most of these genes include binding sites for TFs from the
433 Apetala 2 (AP2), Dof zinc finger protein (C2C2-Dof), and Cysteine-rich Polycomb-like
434 Protein (CPP) families, among others. Binding sites for the single CPP TF, which were
435 highly enriched across all three stress conditions, matched to the promoters of genes from
436 the proline, ASC, and oxidative metabolism pathways, including all four up-regulated
437 copies of *APX* genes. Remarkably, binding sites for the single-enriched Trihelix TF,
438 *Solyc11g012720*, were found only in the promoters of proline metabolism genes.
439 Ultimately, these results suggest that specific sets of TFs coordinate the modulation of
440 proline, ASC, and redox metabolism under salinity + heat stress, which should be further
441 studied to validate their direct or indirect regulatory roles.

442

1
2
3
4
5
6
7
8
9
10
11
12
13
14
15
16
17
18
19
20
21
22
23
24
25
26
27
28
29
30
31
32
33
34
35
36
37
38
39
40
41
42
43
44
45
46
47
48
49
50
51
52
53
54
55
56
57
58
59
60
61
62
63
64
65

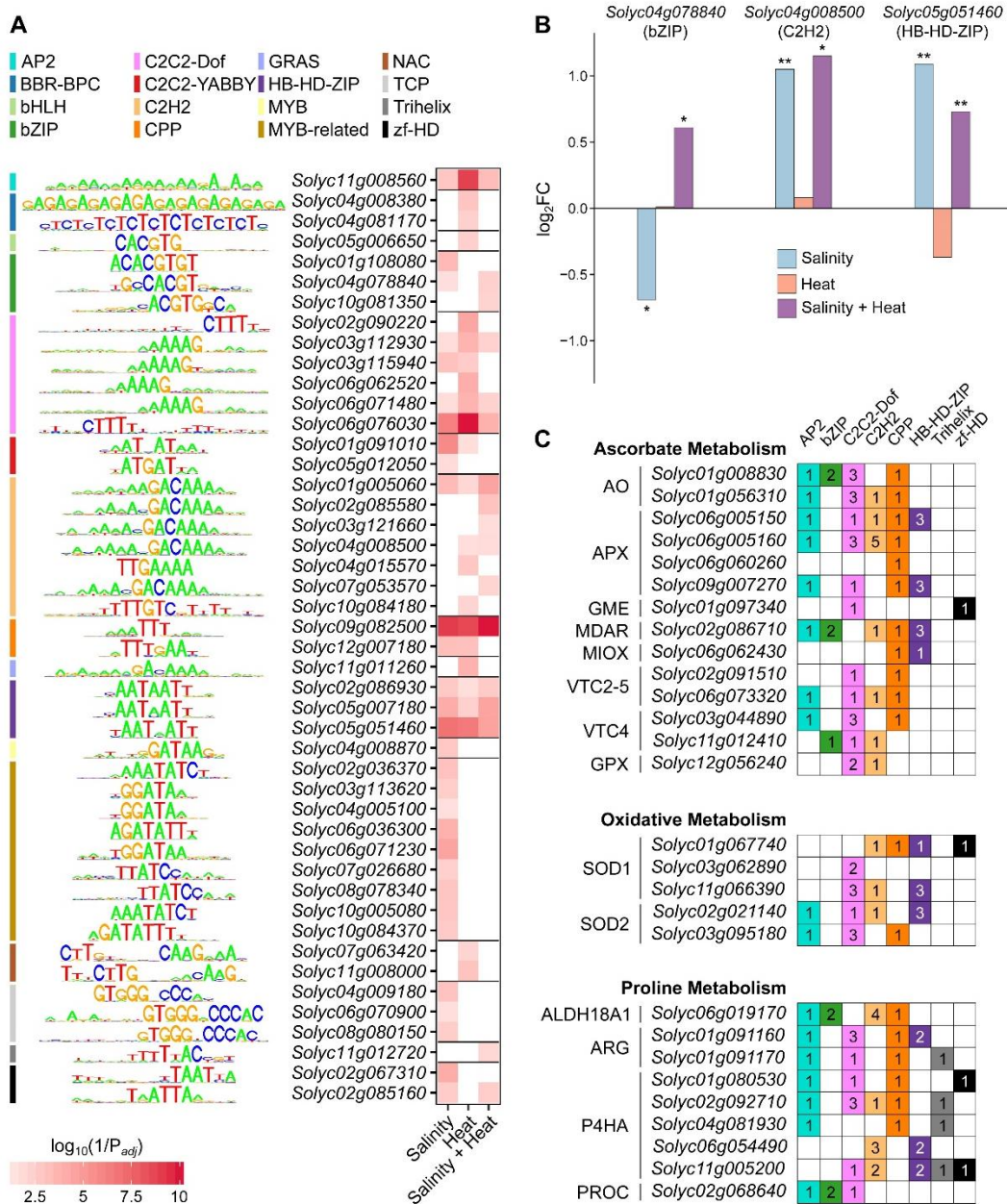


Figure 6. Cis-element enrichment results for up-regulated genes from each stress treatment. **(A)** Enrichment p-values for binding motifs corresponding to 46 TFs in each of the stress treatments. TFs are grouped and color coded by family, and a consensus diagram for the binding motif and gene accession is given for each. **(B)** Log₂(fold change) of expression of three selected TFs in each stress treatment. **(C)** Counts of TF families overrepresented in genes up-regulated in the salinity + heat treatment from the ascorbate metabolism, oxidative metabolism, and proline metabolism families. Accessions and common abbreviations are given for each gene. Numbers in boxes refer to the count of TFs in that family with a match to that gene based on Analysis of Motif Enrichment results.

DISCUSSION

In the present study, we demonstrated that the combination of heat stress with moderate salinity in tomato plants induced a specific physiological, biochemical, and molecular response that could not be deduced from a single stress application. From the

1 449 physiological standpoint, tomato plants under the combination of salinity and heat grew
2 450 better than when salinity was applied as a sole stress, showing a significant increase in
3 451 plant biomass (Fig. 1 A-B). At the same line, plants under stress combination showed
4 452 better photosynthetic performance (Fig. 1 C-F) and lower cellular oxidation than those
5 453 growing under salinity, with the balance between these two processes necessary for both
6 454 plant growth and adaptation to abiotic stress (Considine and Foyer, 2013; Woehle et al.,
7 455 2017). Under salinity stress, ROS accumulation (measured as H₂O₂) likely induced
8 456 damage to membranes and an increase in protein oxidation, which translated into a lower
9 457 cell antioxidant capacity (Fig. 5). These oxidative stress-associated processes may have
10 458 caused the strong inhibition of photosynthesis and reduction of growth observed in plants
11 459 subjected to the salinity treatment. As published previously by our research group (Rivero
12 460 et al. 2014) tomato plants grown under heat stress presented a similar photosynthetic
13 461 performance and values from oxidative markers compared to those grown under control
14 462 conditions. As referred to in Rivero et al. (2014), all the experiments were performed
15 463 under pure hydroponic conditions. Thus, under heat, plants did not close their stomata
16 464 due to water scarcity. Instead, they increased their transpiration rate to lower leaf
17 465 temperature and protect the photosynthetic apparatus. With open stomata and a high
18 466 transpiration rate, the CO₂ assimilation rate continued to be high (similar to control),
19 467 which resulted in plants with similar biomass to control plants. This can also explain the
20 468 values obtained for the oxidative stress-related markers under heat stress, such as H₂O₂
21 469 and MDA, which has been also reported previously by Rivero et al. (2014). Under
22 470 salinity, stomata closed due to the osmotic stress induced by NaCl, which induced a strong
23 471 reduction of the CO₂ assimilation rate, stomatal conductance, and transpiration rate, as
24 472 reported previously by Rivero et al. (2014), leading to an increase in all oxidative stress-
25 473 related markers measured. Thus, and based on the results presented by Rivero et al.
26 474 (2014), Colmenero-Flores and Rosales (2014) indicated that plants have evolved specific
27 475 adaptations to the combination of stresses that do not follow a predictable pattern.
28 476 Interestingly, when salinity was combined with heat, ROS were accumulated to a lesser
29 477 extent, with the damage to membranes and proteins being also lower and maintaining an
30 478 antioxidant capacity of over 60%, which was observed as plants with better growth rates
31 479 than in the salinity conditions alone (Fig. 5). These observations indicate that ROS could
32 480 be produced in a lower quantity under stress combination than under salinity and that
33 481 ROS is being produced at the same level as under salinity, although their detoxification

1
2
3
4
5
6
7
8
9
10
11
12
13
14
15
16
17
18
19
20
21
22
23
24
25
26
27
28
29
30
31
32
33
34
35
36
37
38
39
40
41
42
43
44
45
46
47
48
49
50
51
52
53
54
55
56
57
58
59
60
61
62
63
64
65

482 may be more efficient and/or effective under stress combination. Our results mainly
483 support the latter possibility, in which the combination of salinity and heat-induced the
484 reprogramming of some important stress-related pathways, such as proline and ASC
485 metabolism, facilitating their interconnectivity for a more efficient cellular ROS
486 detoxification through the activation of oxidative metabolism (Fig. 4 and Fig. 5).
487 Tomato plant responses to salinity and heat combination involved complex transcriptional
488 networks and changes in metabolic fluxes. However, the modulation of the proline and
489 ASC pathways was shown to be a strong and unique response to this stress combination.
490 Interestingly, these metabolic pathways were not found to be significantly induced under
491 salinity or heat when applied individually. Proline can protect cells from damage by
492 acting as an osmoprotectant but also as a ROS scavenger (Hossain *et al.*, 2014; Rejeb *et*
493 *al.*, 2014). Although proline metabolism was induced under the combination of salinity
494 and heat, proline levels did not increase under these conditions, and instead, the
495 derivatives 4-hydroxyproline and L-glutamate-5-semialdehyde were significantly
496 accumulated (Fig. 4). Several studies have pointed out that during stress recovery, proline
497 is oxidized to provide the cell with a large amount of energy (one molecule of proline
498 captures 30 ATP equivalents) (Verbruggen and Hermans, 2008; Zhang and Becker,
499 2015). Jaspers and Kangasjärvi (2010) showed that when salinity levels were increased,
500 proline was used as a source of energy by plants, providing ATP and NADPH through its
501 catalysis by the enzyme PRODH. This oxidation process increased the formation of ROS,
502 activating the response signaling cascade generated by the oxidative stress (Jaspers and
503 Kangasjärvi, 2010), and thus relating proline with the stress response mechanisms found
504 in plants.
505 Our results pointed out an interconnection between proline catalysis, ROS generation
506 (due to stress conditions and proline degradation) and an upregulation of the oxidative
507 metabolism (Fig. 4 and Fig. 5). ASC metabolism was also up-regulated, as ASC is a
508 necessary substrate to maintain a balanced oxidative metabolism active. It can be
509 suggested that proline accumulation occurs early during the acclimation to stress
510 combination and that its oxidation is a sign of stress recovery in these plants. However,
511 we have previously reported that proline does not preferentially accumulate during the
512 first 72 hours after tomato plants were subjected to the combination of salinity and heat
513 stress (Rivero *et al.*, 2014), which contradicts this idea. Instead, glycine-betaine was the
514 osmolyte that was preferentially accumulated in tomato under these conditions. Thus, in

1
2
3
4
5
6
7
8
9
10
11
12
13
14
15
16
17
18
19
20
21
22
23
24
25
26
27
28
29
30
31
32
33
34
35
36
37
38
39
40
41
42
43
44
45
46
47
48
49
50
51
52
53
54
55
56
57
58
59
60
61
62
63
64
65

515 this study, we propose and provide evidence that proline oxidation may be interconnected
516 with glutathione redox homeostasis for efficient ROS scavenging. Recent publications
517 have demonstrated that proline catabolism to P5C is induced in animal cells during cell
518 infection (Tang and Pang, 2016). These authors proposed that PRODH and PROC act
519 together to raise P5C levels and thus, govern ROS homeostasis. This mechanism is largely
520 unknown in plants, although a similar hypothesis was proposed in *Arabidopsis thaliana*
521 as a response to pathogen attack (Qamar *et al.*, 2015). In a previous study by our research
522 group (Rivero *et al.*, 2014) we have also shown that PRODH and PROC were
523 differentially up-regulated at the gene and protein levels under the combination of salinity
524 and heat, whereas under salinity or heat applied individually these enzymes were down-
525 regulated, thereby favoring proline accumulation. The significant enrichment of proline
526 metabolism found in the analysis of the transcriptomics and metabolomics data and the
527 potential role of proline intermediaries in ROS homeostasis, such as P5C, provide a strong
528 argument for the role of proline oxidation in ROS signaling mechanisms under stress
529 combination; however, we recognize that more research is needed to confirm this
530 hypothesis.

531 ASC is one of the main compounds involved in plant oxidative metabolism through the
532 Halliwell-Asada cycle, and genes and compounds found in this pathway were
533 significantly induced under salinity and heat combination. Activities of the oxidative
534 metabolism-related enzymes were determined to confirm the upregulation of the
535 oxidative metabolism at the protein level, as well as to find whether or not this pathway
536 was specifically regulated under the combination of salinity and heat, as previously shown
537 for proline and ASC metabolism. Our research group, as well as other authors, have
538 reported on the high activation of oxidative metabolism-related enzymes through a
539 specific upregulation under the combination of salinity in tomato plants (Rivero *et al.*,
540 2014; Martinez *et al.*, 2018; García-Martí *et al.*, 2019). The enzymatic activities assayed,
541 together with the gene expression and the metabolites identified in our study, indicate the
542 efficient detoxification of H₂O₂ through the Halliwell-Asada cycle, and a very active lipid
543 recovery from oxidation thanks to PhGPX activity. These observations could explain that
544 under salinity and heat combination, the oxidative markers measured (H₂O₂, lipid
545 peroxidation, protein oxidation, and antioxidant capacity) in tomato plants were lower
546 than under salinity as the sole stress (Fig. 5).

547 Zandalinas *et al.* (2020) recently described that different combinations of abiotic stresses
548 applied to *A. thaliana* plants resulted in unique transcriptional profiles and that their
549 regulation by different TF families was also characteristic of each stress combination. In
550 this report, the bHLH, MYB and bZIP TFs families were significantly induced under the
551 combination of salinity and heat. Our results showed that some genes belonging to the
552 bZIP TF family were differentially and uniquely regulated under the combination of
553 salinity and heat in tomato plants (e.g., *Solyc10g081350*) (Fig. 6). Other TFs belonging
554 to other stress-related families, such as C2H2 (e.g., *Solyc02g085580*, *Solyc03g121660*,
555 *Solyc07g053570*) and Trihelix (e.g., *Solyc11g012720*), also showed this particularity
556 under our experimental conditions (Fig. 6). Most of these TFs families have been reported
557 to be involved in the control of plant development, cell division, different physiological
558 process, but also in abiotic responses of plants (Kaplan-Levy *et al.*, 2014; Agarwal *et al.*,
559 2019). For example, Agarwal *et al.* (2019) reported that the bZIP family was involved in
560 the mitigation of several abiotic stresses (e.g., salinity, drought, heat or oxidative stress)
561 and the increase in plant productivity under adverse conditions. The Trihelix TF family
562 has been shown to be involved in the response to salinity and pathogen-related stresses,
563 and in the development of trichomes, stomata, and the seed abscission layer (Kaplan-
564 Levy *et al.*, 2014). Numerous members of the C2H2-type zinc finger family have been
565 shown to play a significant role in the plant's response to different abiotic stresses and in
566 plant hormonal transduction signals (Kielbowicz-Matuk, 2012). Most of the information
567 found in the literature regarding the C2H2 family has been for *Arabidopsis*, and very little
568 is known about other plant species, including tomato. Hu *et al.* (2019) found that this
569 family regulates many genes in response to some abiotic stress, and especially in response
570 to heat stress in tomato plants. Most of the C2H2 genes that were up-regulated under heat
571 stress in the report by Hu *et al.* (2019) were also differentially expressed in our
572 transcriptomic analysis when heat was applied as the sole stress (Fig.6). However, the
573 C2H2 identified in our study that was specifically up-regulated under salinity + heat was
574 not listed in the study by Hu *et al.* (2019), again demonstrating the importance of studying
575 stresses in combination. The TFs identified as being up-regulated under the combination
576 of salinity and heat aligned with the promoter regions of many genes studied in this report,
577 including those belonging to the proline, ASC, and oxidative metabolisms.
578 In summary, we showed that proline, ASC and oxidative metabolism are interconnected
579 (Fig. 4), with a tight coordination to maintain not only an optimal cellular redox balance,

1
2
3
4
5
6
7
8
9
10
11
12
13
14
15
16
17
18
19
20
21
22
23
24
25
26
27
28
29
30
31
32
33
34
35
36
37
38
39
40
41
42
43
44
45
46
47
48
49
50
51
52
53
54
55
56
57
58
59
60
61
62
63
64
65

580 but also to trigger the proper signaling mechanisms responsible for inducing the plant's
581 acclimation to the combination of salinity and heat. In this process, proline oxidation is
582 suggested to be used as the energy source needed for triggering the stress response, with
583 subsequent ROS formation (Fig. 5). At this point, oxidative metabolism enters the stage,
584 with the upregulation of its main enzymes to maintain ROS at basal levels. One of the
585 main limiting factors for maintaining the activity of the redox metabolic pathways is ASC
586 abundance, which suggests the presence of a connection between ASC biosynthesis with
587 oxidative metabolism and, most likely, with proline oxidation. Cellular basal levels of
588 ROS could trigger downstream signaling mechanisms through the activation of particular
589 TFs families, such as the trihelix, C2H2 and bZIP families, which in turn, may regulate
590 the expression of genes involved in the reprogramming of different metabolic pathways,
591 including those involved in proline, ASC, and redox metabolism (i.e., positive feedback
592 loops). Future validation of the role of specific TFs families in the successful acclimation
593 of plants to heat + salinity is necessary for developing breeding strategies for more
594 resilient crops against abiotic stresses.

595

596 **Supplementary data**

597 **Figure S1.** Total ion chromatogram extracted from UPLC-QTOF performed in 6
598 biological replications of tomato leaves subjected to control, salinity heat or the
599 combination of salinity + heat.

600 **Figure S2.** Box-and-whisker plots of the compounds belong to the Ascobate, aldarate and
601 oxidative metabolism with significant differences between salinity + heat treatment
602 respect to control.

603 **Figure S3.** Box-and-whisker plots of the compounds belong to the Proline metabolism
604 with significant differences between salinity + heat treatment with respect to control.

605 **Table S1.** Raw, parsed and mapped reads of mRNA of all samples.

606 **Table S2 - Sheet 1-** Comparison of salinity-treated tomato plants against control plants.

607 **Sheet 2-** Comparison of heat-treated tomato plants against control plants. **Sheet 3-**

608 Comparison of the salinity combined with heat treatment against control plants.

609 **Table S3.** Comparison of the peaks of each independent analysis with the aim of finding
610 common and specific peaks among all the treatments.

611 **Table S4.** Identified compounds in the Control vs Salinity+Heat peaks comparison
612 related to the enriched pathway analysis results.

613 **Table S5.** Activities of the oxidative metabolism-related enzymes.

614 **Table S6.** Differential expression output from DESeq2 (Love et al., 2014).

615 **Table S7.** Enrichment of KEGG pathways in upregulated genes for each treatment.

616

617 **Data availability:** The raw sequencing reads and the read mapping count matrices are
618 available in the National Center for Biotechnology Information Gene Expression
619 Omnibus database under the accession GSE152620. All data supporting the findings of
620 this study are available within the paper and within its supplementary materials published
621 online.

622

623 **Acknowledgments**

624 This work was supported by the Ministry of Economy and Competitiveness from Spain
625 (Grant No. PGC2018-09573-B-100) to R.M.R (Murcia, Spain), by the Ministry of
626 Science, Innovation and Universities of Spain (Grant No. FPU16/05265) to M.L-D.
627 (Murcia, Spain) and by start-up funds from the College of Agricultural and Environmental
628 Sciences and the Department of Plant Sciences (UC Davis) to B.B-U (Davis, CA, United
629 States). We sincerely acknowledge Mario G. Fon for proof-reading the manuscript. We
630 also thank the Metabolomics Core of CEBAS-CSIC for the assistance with the analysis.
631 All authors declare no commercial, industrial links or affiliations.

632

633 **Author contribution**

634 RMR conceived, designed and supervised the experiments; ML-D, CJS and BB-U
635 performed the RNAseq analysis. VM and RMR performed the metabolomic analysis.
636 ML-D, TCM and RMR performed the biochemical analysis. ML-D and RMR performed
637 the photosynthetic measurements. ML-D, BB-U and RMR wrote the paper. The authors
638 declare that they have no competing interests.

639

640 **References**

641 **Aebi H.** 1984. Catalase in Vitro. *Methods in Enzymology* **105**, 121–126.

642 **Agarwal P, Baranwal VK, Khurana P.** 2019. Genome-wide Analysis of bZIP
643 Transcription Factors in wheat and Functional Characterization of a TabZIP under
644 Abiotic Stress. *Scientific Reports* **9**, 4608.

645 **Akram NA, Shafiq F, Ashraf M.** 2017. Ascorbic acid-a potential oxidant scavenger and

1
2
3
4
5
6
7
8
9
10
11
12
13
14
15
16
17
18
19
20
21
22
23
24
25
26
27
28
29
30
31
32
33
34
35
36
37
38
39
40
41
42
43
44
45
46
47
48
49
50
51
52
53
54
55
56
57
58
59
60
61
62
63
64
65

646 its role in plant development and abiotic stress tolerance. *Frontiers in Plant Science* **8**.

647 **Anjum SA, Xie X-Y, Wang L-C, Saleem MF, Man C, Lei W.** 2019. Morphological,
648 physiological and biochemical responses of plants to drought stress. *African Journal of*
649 *Agricultural Research* **6**.

650 **Benjamini Y, Hochberg Y.** 1995. Controlling the False Discovery Rate: A Practical and
651 Powerful Approach to Multiple Testing. *Journal of the Royal Statistical Society: Series*
652 *B (Methodological)* **57**, 289–300.

653 **Bolger AM, Lohse M, Usadel B.** 2014. Trimmomatic: a flexible trimmer for Illumina
654 sequence data. *Bioinformatics (Oxford, England)* **30**, 2114–2120.

655 **Bradford MM.** 1976. A rapid and sensitive method for the quantitation of microgram
656 quantities of protein utilizing the principle of protein-dye binding. *Analytical*
657 *Biochemistry* **72**, 248–254.

658 **Castelán-Muñoz N, Herrera J, Cajero-Sánchez W, Arrizubieta M, Trejo C, García-**
659 **Ponce B, Sánchez M de la P, Álvarez-Buylla ER, Garay-Arroyo A.** 2019. MADS-box
660 genes are key components of genetic regulatory networks involved in abiotic stress and
661 plastic developmental responses in plants. *Frontiers in Plant Science* **10**.

662 **Colmenero- Flores JM, Rosales MA.** 2014. Interaction between salt and heat stress.
663 *Plant Cell Environ*, **37**: 1042-1045.

664 **Considine MJ, Foyer CH.** 2013. Redox Regulation of Plant Development. *Antioxidants*
665 *& Redox Signaling* **21**, 1305–1326.

666 **Foyer CH, Noctor G.** 2011. Ascorbate and glutathione: The heart of the redox hub. *Plant*
667 *Physiology* **155**, 2–18.

668 **Fu J, Huang B.** 2001. Involvement of antioxidants and lipid peroxidation in the
669 adaptation of two cool-season grasses to localized drought stress. *Environmental and*
670 *Experimental Botany* **45**, 105–114.

671 **García-Martí M, Piñero MC, García-Sánchez F, Mestre TC, López-Delacalle M,**
672 **Martínez V, Rivero RM.** 2019. Amelioration of the Oxidative Stress Generated by
673 Simple or Combined Abiotic Stress through the K⁺ and Ca²⁺ Supplementation in Tomato
674 Plants. *Antioxidants* **8**, 81.

675 **Halliwell B, Foyer CH.** 1976. *Ascorbic Acid, Metal Ions and the Superoxide Radical*.

676 **Hoagland DR, Arnon DI.** 1950. The water-culture method for growing plants without
677 soil. Circular. California Agricultural Experiment Station **347**.

678 **Hossain MA, Hoque MA, Burritt DJ, Fujita M.** 2014. Chapter 16 - Proline Protects

679 Plants Against Abiotic Oxidative Stress: Biochemical and Molecular Mechanisms, In:
680 Oxidative Damage to Plants, Ed(s): Parvaiz Ahmad, Academic Press, pp: **477-522**

681 **Hu X, Zhu L, Zhang Y, Xu L, Li N, Zhang X, Pan Y.** 2019. Genome-wide
682 identification of C2H2 zinc-finger genes and their expression patterns under heat stress
683 in tomato (*Solanum lycopersicum* L.) (G Sun, Ed.). *PeerJ* **7**, e7929.

684 **Jaspers P, Kangasjärvi J.** 2010. Reactive oxygen species in abiotic stress signaling.
685 *Physiologia Plantarum* **138**, 405–413.

686 **Kaplan-Levy RN, Quon T, O'Brien M, Sappl PG, Smyth DR.** 2014. Functional
687 domains of the PETAL LOSS protein, a trihelix transcription factor that represses
688 regional growth in *Arabidopsis thaliana*. *The Plant Journal* **79**, 477–491.

689 **Kielbowicz-Matuk A.** 2012. Involvement of plant C2H2-type zinc finger transcription
690 factors in stress responses. *Plant Science* **185–186**, 78–85.

691 **Koleva II, van Beek TA, Linssen JPH, Groot A de, Evstatieva LN.** 2002. Screening
692 of Plant Extracts for Antioxidant Activity: a Comparative Study on Three Testing
693 Methods. *Phytochemical Analysis* **13**, 8–17.

694 **Kollist H, Zandalinas SI, Sengupta S, Nuhkat M, Kangasjärvi J, Mittler R.** 2019.
695 Rapid Responses to Abiotic Stress: Priming the Landscape for the Signal Transduction
696 Network. *Trends in Plant Science* **24**, 25–37.

697 **Langmead B, Salzberg SL.** 2012. Fast gapped-read alignment with Bowtie 2. *Nature*
698 *methods* **9**, 357–359.

699 **Lopez-Delacalle M, Camejo D, ... MG-M-F in P, 2019 U.** 2020. Using tomato
700 recombinant lines to improve plant tolerance to stress combination through a more
701 efficient nitrogen metabolism. *Frontiers*.

702 **Love MI, Huber W, Anders S.** 2014. Moderated estimation of fold change and
703 dispersion for RNA-seq data with DESeq2. *Genome Biology* **15**, 550.

704 **MacNevin WM, Urone PF.** 1953. Separation of Hydrogen Peroxide from Organic
705 Hydroperoxides. *Analytical Chemistry* **25**, 1760–1761.

706 **Martinez V, Mestre TC, Rubio F, Girones-Vilaplana A, Moreno DA, Mittler R,**
707 **Rivero RM.** 2016. Accumulation of flavonols over hydroxycinnamic acids favors
708 oxidative damage protection under abiotic stress. *Frontiers in Plant Science* **7**.

709 **Martinez V, Nieves-Cordones M, Lopez-Delacalle M, Rodenas R, Mestre TC,**
710 **Garcia-Sanchez F, Rubio F, Nortes PA, Mittler R, Rivero RM.** 2018. Tolerance to
711 stress combination in tomato plants: New insights in the protective role of melatonin.

712 Molecules **23**, 1–20.

1
2 713 **McCord JM FI**. 1969. The utility of superoxide Dismutase in studying free Radicals
3 714 Reactions. The Journal of biological chemistry **244**, 6056 – 63.

4
5 715 **McLeay RC, Bailey TL**. 2010. Motif Enrichment Analysis: a unified framework and an
6 716 evaluation on ChIP data. BMC Bioinformatics **11**, 165.

7
8 717 **Meyer AJ**. 2008. The integration of glutathione homeostasis and redox signaling. Journal
9 718 of Plant Physiology **165**, 1390–1403.

10
11 719 **Miller G, Suzuki N, Ciftci-Yilmaz S, Mittler R**. 2010. Reactive oxygen species
12 720 homeostasis and signalling during drought and salinity stresses. Plant, Cell and
13 721 Environment **33**, 453–467.

14
15 722 **Mittler R**. 2006. Abiotic stress, the field environment and stress combination. Trends in
16 723 Plant Science.

17
18 724 **Miyake C, Asada K**. 1992. Thylakoid-Bound Ascorbate Peroxidase in Spinach
19 725 Chloroplasts and Photoreduction of Its Primary Oxidation Product
20 726 Monodehydroascorbate Radicals in Thylakoids. Plant and Cell Physiology **33**, 541–553.

21
22 727 **Moriya Y, Itoh M, Okuda S, Yoshizawa AC, Kanehisa M**. 2007. KAAS: an automatic
23 728 genome annotation and pathway reconstruction server. Nucleic Acids Research **35**,
24 729 W182–W185.

25
26 730 **Nieves-Cordones M, López-Delacalle M, Ródenas R, Martínez V, Rubio F, Rivero**
27 731 **RM**. 2019. Critical responses to nutrient deprivation: A comprehensive review on the role
28 732 of ROS and RNS. Environmental and Experimental Botany **161**, 74–85.

29
30 733 **Noctor G, Foyer CH**. 1998. ASCORBATE AND GLUTATHIONE: Keeping Active
31 734 Oxygen Under Control. Annual Review of Plant Physiology and Plant Molecular Biology
32 735 **49**, 249–279.

33
34 736 **Qamar A, Mysore KS, Senthil-Kumar M**. 2015. Role of proline and pyrroline-5-
35 737 carboxylate metabolism in plant defense against invading pathogens. Frontiers in plant
36 738 science **6**, 503.

37
38 739 **Rejeb KB, Abdelly C, Savouré A**. 2014. How reactive oxygen species and proline face
39 740 stress together. Plant Physiology and Biochemistry **80**, 278-284.

40
41 741 **Reznick AZ, Packer L**. 1994. [38] Oxidative damage to proteins: Spectrophotometric
42 742 method for carbonyl assay. Methods in Enzymology. Academic Press, 357–363.

43
44 743 **Rivera A, Bravo C, Buob G**. 2017. *Climate Change and Land Ice*.

45
46 744 **Rivero RM, Mestre TC, Mittler R, Rubio F, Garcia-Sanchez F, Martinez V**. 2014.

1
2
3
4
5
6
7
8
9
10
11
12
13
14
15
16
17
18
19
20
21
22
23
24
25
26
27
28
29
30
31
32
33
34
35
36
37
38
39
40
41
42
43
44
45
46
47
48
49
50
51
52
53
54
55
56
57
58
59
60
61
62
63
64
65

1
2
3
4
5
6
7
8
9
10
11
12
13
14
15
16
17
18
19
20
21
22
23
24
25
26
27
28
29
30
31
32
33
34
35
36
37
38
39
40
41
42
43
44
45
46
47
48
49
50
51
52
53
54
55
56
57
58
59
60
61
62
63
64
65

745 The combined effect of salinity and heat reveals a specific physiological, biochemical and
746 molecular response in tomato plants. *Plant, Cell and Environment* **37**, 1059–1073.

747 **Rivero RM, Ruiz JM, Romero L.** 2004a. Oxidative metabolism in tomato plants
748 subjected to heat stress. *Journal of Horticultural Science and Biotechnology* **79**, 560–564.

749 **Rivero RM, Ruiz JM, Romero LM.** 2004b. Importance of N source on heat stress
750 tolerance due to the accumulation of proline and quaternary ammonium compounds in
751 tomato plants. *Plant Biology* **6**, 702–707.

752 **Sayed HESA El.** 2013. Exogenous application of ascorbic acid for improve germination,
753 growth, water relations, organic and inorganic components in tomato (*Lycopersicon*
754 *esculentum* Mill.). *New York Science Journal* **6**, 123–139.

755 **Schmidt R, Schippers JHM, Welker A, Mieulet D, Guiderdoni E, Mueller-Roeber**
756 **B.** 2012. Transcription factor *osh5c1b* regulates salt tolerance and development in *oryza*
757 *sativa* ssp. *japonica*. *AoB PLANTS* **12**.

758 **Sehgal A, Sita K, Bhandari K, Kumar S, Kumar J, Vara Prasad P V, Siddique**
759 **KHM, Nayyar H.** 2019. Influence of drought and heat stress, applied independently or
760 in combination during seed development, on qualitative and quantitative aspects of seeds
761 of lentil (*Lens culinaris* Medikus) genotypes, differing in drought sensitivity. *Plant Cell*
762 *and Environment* **42**, 198–211.

763 **Shalata A, Neumann PM.** 2001. Exogenous ascorbic acid (vitamin C) increases
764 resistance to salt stress and reduces lipid peroxidation. *Journal of Experimental Botany*
765 **52**, 2207–2211.

766 **Suzuki N, Koussevitzky S, Mittler R, Miller G.** 2012. ROS and redox signalling in the
767 response of plants to abiotic stress. *Plant, Cell and Environment* **35**, 259–270.

768 **Tang H, Pang S.** 2016. Proline Catabolism Modulates Innate Immunity in
769 *Caenorhabditis elegans*. *Cell Reports* **17**, 2837–2844.

770 **Torres CA, Andrews PK, Davies NM.** 2006. Physiological and biochemical responses
771 of fruit exocarp of tomato (*Lycopersicon esculentum* Mill.) mutants to natural photo-
772 oxidative conditions. *Journal of Experimental Botany*.1933–1947.

773 **Verbruggen N, Hermans C.** 2008. Proline accumulation in plants: a review. *Amino*
774 *Acids* **35**, 753–759.

775 **Woehle C, Dagan T, Landan G, Vardi A, Rosenwasser S.** 2017. Expansion of the
776 redox-sensitive proteome coincides with the plastid endosymbiosis. *Nature Plants* **3**,
777 17066.

1
2 778 **Zandalinas SI, Fritschi FB, Mittler R, Lawson T.** 2020. Signal transduction networks
779 during stress combination. *Journal of Experimental Botany* **71**, 1734–1741.

3
4 780 **Zhang L, Becker D.** 2015. Connecting proline metabolism and signaling pathways in
5 781 plant senescence. *Frontiers in Plant Science* **6**, 552.

6
7 782 **Zushi K, Ono M, Matsuzoe N.** 2014. Light intensity modulates antioxidant systems in
8 783 salt-stressed tomato (*Solanum lycopersicum* L. cv. Micro-Tom) fruits. *Scientia*
9 784 *Horticulturae* **165**, 384–391.

10
11 785

12
13 786

14
15
16 787 **Figure Legends**

17
18 788 **Figure 1.** (A) Pictures of tomato plants at the end of the control or stress treatments. (B)
19
20 789 Whole plant fresh weight (FW) of tomato plants grown under control, heat, salinity
21
22 790 or the combination of salinity and heat. (C-F) Photosynthetic parameters measured
23
24 791 in the third and four fully mature expanded leaves of tomato plants grown under
25
26 792 control or stress conditions measured at the beginning (0 days), during (7 days) or at
27
28 793 the end (14 days) of the treatments. Values represent means \pm SE (n = 9). Bars with
29
30 794 different letters within each panel are significantly different at $p < 0.05$ according to
31
32 795 Tukey's test. WUE: water use efficiency; DOT: days of treatment.

33 796 **Figure 2.** RNAseq analysis performed in tomato leaves after 14 days of growing under
34
35 797 control or stress (salinity, heat or the combination of salinity and heat) conditions.
36
37 798 (A) Principal component analysis (PCA) of the normalized reads obtained for each
38
39 799 treatment. (B) Euler diagram representing up- and down-regulated genes (adjusted
40
41 800 $P < 0.05$) of tomato plants grown under control, simple (salinity or heat) or combined
42
43 801 (salinity + heat) stress. (C) Pathway enrichment analysis performed within the up-
44
45 802 regulated genes under the different stress conditions applied. The scale is the
46
47 803 $\log_{10}(1/P_{adj})$, with redder colors indicating greater statistical significance. Values
48
49 804 greater than 10 were converted to 10 for scaling purposes. More details on these
50
51 805 analyses can be found in the Materials and Method section.

52
53 806 **Figure 3.** Metabolomic analysis performed in tomato leaves after 14 days of growing
54
55 807 under control, simple (salinity or heat) or combined (salinity + heat) stress
56
57 808 conditions. (A) Principal component analysis (PCA) of the normalized molecular
58
59 809 features found under each treatment applied (n = 6). (B) Euler diagram of the
60
61 810 common and uniquely molecular features with a differential and significant

62
63
64
65

1
2
3
4
5
6
7
8
9
10
11
12
13
14
15
16
17
18
19
20
21
22
23
24
25
26
27
28
29
30
31
32
33
34
35
36
37
38
39
40
41
42
43
44
45
46
47
48
49
50
51
52
53
54
55
56
57
58
59
60
61
62
63
64
65

811 accumulation in each treatment ($P_{adj} < 0.05$). (C) Bubble diagram representing the
812 up- and down-regulated molecular features found among the 568 molecular features
813 uniquely and significantly changing under the combination of salinity + heat. Each
814 bubble (i.e. molecular feature) is positioned in the chromatogram by its mass-to-
815 charge (y-axis) and retention time (x-axis) and the size and darkness of one bubble
816 represented the \log_2 and p-value, respectively of this molecular feature. The raw data
817 of Figure 3C can be found in the supplementary material (Supplementary Table S2
818 and S3). (D) KEGG pathway enrichment analysis performed with the significantly
819 up-regulated molecular features identified under the combination of salinity + heat.
820 More details on these analyses can be found in the Materials and Methods section.

821 **Figure 4.** Schematic diagram of the metabolic interconnection between ascorbate, proline
822 and oxidative metabolism in tomato plants. \log_2 (fold change) of the metabolite
823 concentration (\circ), gene expression (\square) or enzymatic activity (\diamond) obtained in tomato
824 plants grown under the combination of salinity + heat after RNAseq, metabolomics
825 or biochemical analyses were represented. The data represented for genes,
826 metabolites and enzymatic activities were obtained by comparison with the control
827 treatment. Row data and specific information can be found in Material and Methods
828 section and in the Supplementary material.

829 **Figure 5.** Oxidative metabolism-related markers measured in tomato leaves grown for 14
830 days under control, simple (salinity +heat) or combined (salinity+heat) stress. Values
831 represent means \pm SE (n = 9). Bars with different letters within each panel are
832 significantly different at $p < 0.05$ according to Tukey's test.

833 **Figure 6.** Cis-element enrichment results for up-regulated genes from each stress
834 treatment. (A) Enrichment p-values for binding motifs corresponding to 46 TFs in
835 each of the stress treatments. TFs are grouped and color-coded by family, and a
836 consensus diagram for the binding motif and gene accession is given for each. (B)
837 \log_2 (fold change) of expression of three selected TFs in each stress treatment. (C)
838 Counts of TF families overrepresented in genes up-regulated in the salinity + heat
839 treatment from the ascorbate metabolism, oxidative metabolism, and proline
840 metabolism families. Accessions and common abbreviations are given for each gene.
841 Numbers in boxes refer to the count of TFs in that family with a match to that gene
842 based on Analysis of Motif Enrichment results.ç